Integrating Core and Aeromagnetic Datasets to Evaluate Mineral Potential of Southern Nupe Basin, Nigeria

Ayatu Usman (ayatuusman@gmail.com)
Alex Ekwueme Federal University, Ndufu-Alike, Ikwo, Ebonyi, Nigeria
Geogerbest Azuoko
Alex Ekwueme Federal University, Ndufu-Alike, Ikwo, Ebonyi, Nigeria
Joshua Chizoba
Alex Ekwueme Federal University, Ndufu-Alike, Ikwo, Ebonyi, Nigeria
Ifeanyi Chinwuko
Nnamdi Azikiwe University

Research Article

Keywords: Aeromagnetic data, Core data, Spectral analysis, Curie isotherm, Oolitic Iron or

Posted Date: January 14th, 2022

DOI: https://doi.org/10.21203/rs.3.rs-1227915/v1

Abstract

Aeromagnetic and core drilled data covering parts of southern Nupe Basin was acquired and interpreted with the view to evaluating the mineral potentials of the area through interpretation of the structural features in the area; determination of the curie isotherm depth; and correlation of aeromagnetic outcomes with the core sample data from the area. Two major regional fault trends were interpreted, trending, Northeast–Southwest (NE–SW) and NNE–SSW with minor northwest–southeast (NW–SE) directions. Two depth sources in the area are delineated namely; zone of shallow seated basement which ranges from 0.42km to 1.5km and zone of deeply seated basement which ranges from 1.91 to 3.50km.Results of qualitative interpretation of the Total magnetic intensity map (TMI) and Residual intensity map reveal that the magnetic intensities ranges from 7500 to 8460 nano-Telsa (nT) and -220 to 240 nT respectively. The depth to the centroid and top of the magnetic caustic bodies ranges from 9.00 to 17.10km and 0.4 to 3.10km respectively. Juxtaposing the topographical and core drilling data reveals that the oolitic iron ore level follows the topographical level which implies that the topography of the area controls the configuration of the iron ore deposit level. All these deduction are made considering the geology of the area.

1. Introduction

The study area is situated within the Nupe Basin also called the Mid Niger Basin. It is an intracratonic basin extending from Kontagora in Niger State to areas slightly beyond Lokoja in the south (Obaje et al, 2013) (Fig. 2 and 3). It lies between latitudes 8^{o} 00^{l} N- 9^{o} 30^{l} N and longitudes 5^{o} 30^{l} E- 7^{o} 00^{l} E (Fig. 1) and some noted town there include: Bida, Paiko, Pategi, Baro, Gulu, Isanlu, Aiyegunle, Kotonkarfi and Birin. The study area was chosen because of its interesting feature and interest of the researchers in Sedimentary/Basement contact.

Aeromagnetic survey routinely target caustic magnetic bodies that poses unusual characteristic which mostly reveals themselves in form of anomalies. Magnetic properties are predominating in basement rocks and minimum in sedimentary rocks. According to Onwuemesi, (1995 and 1997) and also Anakwuba and Chinwuko (2015), delineation of the subsurface requires a more advanced technique which the magnetic survey provides. These techniques can comfortably help in mapping the subsurface structures, calculate the depth parameter and model them because it is a fast, target oriented and cost effective geophysical method.

The works of some notable authors such as Singh and Biswas (2016), Saibi et al, (2015) Bhattacharyya and Leu, (1975), (Ross et al, 2006; Mandal, et al, 2013; Abraham et al., 2014) suggested that Curie isotherm and geothermal gradients can be used to complement geothermal data information in an areas where borehole information are not available. And this study is not an exception, as it attempt to integrate aeromagnetic and core data to evaluate the mineral potential of the basin.

This research work focuses on the Evaluation of the mineral potential of the Nupe basin, through the use of centroid and forward modelling of the spectral peak methods, over some parts of southern Nupe Basin, North- Central Nigeria. This will delineate the geometry of the basin by evaluating the basal depth of the caustic magnetic rock, the thickness of the magnetic basement and crustal temperature information in the area of study. It will also reveal the geologic structures and possibly provide a 3D model of the basin.

2. Geological Setting

The stratigraphic sequence of the Nupe Basin, are referred to as the Bida Group (Adeleye, 1973), it is sub divided into Northern Nupe Basin (Sub-Basin) and Southern Nupe Sub-Basin or Lokoja Sub-Basin (Fig. 2). The Nupe Basin is presumed to be a north-western extension of the Anambra Basin (Akande et al., 2005). The basin fill contains a cretaceous sediment that were believed to be deposited as a result of, subsidence, rifting, block faulting, basement fragmentation and drifting resultant to the Cretaceous inaugural of the South Atlantic Ocean. The main parallel movements laterally to the north-eastern to south-western axis of the adjacent Benue Trough seems to have been interpreted to the north-south and north-western trending shear region to form the Mid-Niger Basin abrupt to the Benue Trough (Ojonugwa *et al.*, 2018).

Nupe basin is an extension of the Anambra basin but it was subdivided in the Santonian. There is an accumulation of Pre-Santonian sediment in the lower Benue Trough and the adjacent southern Anambra basin. Obaje et al, 2013 recorded that the Nupe basin and the southern Anambra basin platform collapse and this led to sedimentation of the upper cretaceous depositional cycle which begins with the accumulation of the marine shales (the Nkporo shale and Enugu shale Formations). These Formations is believed to have some lateral equivalent with the Lokoja Formation of the Nupe Basin (Obaje et al, 2013).

The Mamu Formation of the southern Anambra Basin underlies the Nkporo shale Formation. Lithologically the Mamu Formation comprises of sandstone, siltstone with shale intercalation and coal seal deposit of deltaic to estuarine environments. Its lateral equivalent is the Bida Formation in the Nupe Basin (Obaje et al, 2013). The Ajali Sandstone Formation underlies the Mamu Formation and it lateral equivalent is the Patti, Sakpe and Enagi Formations of the Nupe Basin (Fig. 3). The predominant lithic component of this formation is well sorted sandstone. This sandstone is commonly interbeded with claystone and siltstone. This is eminent in Patti Formation. Agbaja iron Formation and Batati Formation are iron rich, they overlies the Patti and Batati Formation (Fig. 3).

3. Methodology

The input data's used in the study are nine aeromagnetic data namely; [Sheets- 183 (Egbako), 184 (Bida), 185 (Paiko), 204 (Pategi), 246 (Baro), 206 (Gulu), 225 (Isanlu), 226 (Aiyegunle) and 227 (Kotonkarfi)] and core drilled data. The aeromagnetic sheets were assembled, analysed and digitised on a scale of 1: 100,000 and the total surveyed are is 27,225 square kilometers. The aeromagnetic data was enhanced using mathematical filters such as downward continuation, upward continuation, first vertical derivative,

analytical signal and reduction to the pole. For we to interpret the local body, the enhanced data is separated into religion field and the residual field using the multiple regression techniques. The input data used for the spectral analysis is the residual data and it helps in evaluation of depth to the magnetic sources; delineate Curie isotherm temperature and heat flow. Hence, the residual data were subjected to both graphical and mathematical modelling for quantitative interpretation, this help us to deduce the thermomagnetic properties in the area.

The borehole data obtained is the Enegbaki - Akpogu Oolitic iron ore deposit is situated at about 9km North East of Akpogu village which lies along Lokoja- Abuja Road. The deposit being investigated has an area of 1.0 sq.km and is capped by lateritic top layer, clay and some silica. The iron ore bearing plateau trends in a NE – SW direction with an average height of 263m above sea level. Twenty-five (25) core holes placed at 250m grid interval were drilled using rotary type of drilling (Massenza Multipurpose drill).

Qualitatively interpretations were done using visual inspection of the total magnetic field data, residue field data and analytical signal map of the area. More so, core data were analysed and interpreted in order to produce the oolitic iron model in the area. Lastly, areas with geothermal energy potential were delineated using integrated geological and geophysical data. The workflow is shown in Fig. 4.

4. Results And Discussion

The total magnetic intensity (TMI) and residual anomaly maps (Fig. 5 and Fig. 6) were contoured from the digitized data. Visual assessment of the TMI and residual anomalous maps reveals intricate form of magnetic signatures of both short and long wavelengths (Fig. 5 and Fig. 6), this is an indication of variable magnetic intensities from diverse geologic sources as supported by the work of Okonkwo et al. (2012) and these variable magnetic intensities is well pronounced in the study area. The mangetic intensity values of the TMI and residual anomalous maps ranges from 7800 to 8200 nT and -220 to 240 nT respectively (Fig. 5 and 6). There are strong evidences of igneous intrusion when juxtaposed with the geologic map of the area. These intrusions account for the high level of faulting and folding around the study area.

More so, these areas mentioned above possess mostly close-spaced contour lines and this implies thinner sedimentary infillings (that is the depth to the top of the basement is shallow); Again, oval contours also encounter in this area may also be an indication of intrusive igneous bodies or lineaments containing groups of mineral deposit of great economic values as evident in the study area like Koton-Karfi, Abaji, Bida and Paiko.

At the central parts (Pategi, Baro, Gulu, Lafiagi) of the study area,contains widely spaced contour, signifying thick sedimentary infilling (that is deeper magnetic sources) within these areas (Fig. 5). It is therefore logical to conclude that the widely spaced contours in conjunction with the high magnetic intensity values detected in the area may have been related with a vein bearing mineral this assertion is supported by the geologic map of the study (Fig. 7 and 8).

The structural alignment of the area was evaluated using the anomalous residual shaded maps (Fig. 9) produced from the residual acoustic field intensity map. The major trend of the lineament were NE-SW and minor ones trending E-W and NW-SE. This structural direction is in conformity with previous work by (Chinwuko, et al 2012, 2014 and Ojonugwa, et al 2018). There are high lineament concentration which suggests intense tectonic activities that affected the deeply seated basement rock and it's abutting Cretaceous sequences. According to previous works such as Abraham et al, (2014), Ojonugwa et al (2018); Obaje et al. (2013) propose that the NE-SW NNE-SSW and NW-SE within the study area are regarded as Pan-African Orogeny while the E-W may probably have been Pre-Pan-African Orogeny. The structures can serve as migrating path for geothermal and fluid.

The residual magnetic anomalies data were subjected to both Peter's half-slope method and spectral analysis for depth calculation (sedimentary thicknesses) and depth modelling within the study area (Fig. 10). The result of the analysis is shown in Table 1. The interpreted result reveals two-layer depth model; the shallower magnetic depth bodies which varies from 0.54 to 1.87km (for Peter's slope method), and 1.27 to 1.96km; for spectral analysis interpretation, deeper magnetic bodies of depth range of 2.01 to 3.27km (for Peter's slope method) and 2.01 to 4.27km for spectral analysis. Again, the depth to the centroid obtained through the spectral analysis reveals depth range of 9.79 to 15.75km across the area (Table 1).

Table 1
Depth calculation using Spectral Analysis

	Spectral Analysis **Peter's Slope method**		**Peter's Slope method**			
Anomaly	Depth to Top Of Basement Z_t (km)	Depth to Botton of Basement Z_p (km)	Z_o (km)	Curie Point Depth (km)	dT/dZ (^oC/km)	q(mWm2)
1	2.09	1.86	14.73	27.37	24.733	61.834
2	3.11	2.41	12.84	22.57	28.046	70.116
3	1.49	2.88	15.11	28.73	23.359	58.397
4	0.96	0.56	13.45	25.94	24.380	60.950
5	2.42	2.64	12.88	23.34	28.238	70.594
6	3.18	2.93	10.06	16.94	23.191	57.977
7	3.05	2.71	13.92	24.79	23.800	59.499
8	1.52	1.83	12.87	24.22	26.197	65.492
9	1.14	2.05	14.31	27.48	28.798	71.996
10	1.08	2.61	12.95	24.82	20.781	51.953
11	0.53	2.28	16.28	32.03	25.043	62.608
12	2.46	1.42	12.21	21.96	25.641	64.103
13	3.22	2.33	11.04	18.86	22.516	56.289
14	3.07	2.39	14.53	25.99	23.761	59.402
15	1.49	1.71	16.84	32.19	30.240	75.600
16	0.45	2.14	15.06	29.67	28.087	70.2179
17	2.71	3.27	13.01	23.31	24.545	61.363
18	3.24	1.81	9.09	14.94	26.316	65.789
19	3.19	2.96	11.23	19.27	24.017	60.041
20	2.85	2.57	13.69	24.53	24.618	61.545

	Spectral Analysis Peter's Slope method		Peter's Slope method			
21	2.25	1.74	14.47	26.69	24.733	61.834
22	2.33	1.71	12.61	22.89	27.154	67.884
23	2.08	2.01	11.89	21.7	26.839	67.099
24	2.86	2.11	14.05	25.24	24.670	61.676
25	3.23	2.42	13.11	22.99	25.709	64.273
26	2.98	1.72	9.47	15.96	26.902	67.254
27	1.81	1.79	13.22	24.63	22.222	55.556
28	1.65	0.78	16.51	31.37	21.978	54.945
29	2.13	0.83	14.83	27.53	24.278	60.695
30	3.17	2.15	16.32	29.47	24.116	60.291
31	3.22	1.44	11.63	20.04	23.761	59.402
32	2.08	0.76	13.83	25.58	26.364	65.909
33	2.01	1.96	12.94	23.87	30.950	77.375
34	2.14	1.38	15.77	29.4	25.483	63.708
35	2.33	1.97	13.22	24.11	24.744	61.860
36	2.79	2.38	15.64	28.49	23.043	57.608
37	2.47	1.16	14.85	27.23	27.397	68.493
Average	2.29135135	2.01	13.52594595	24.76054054	25.277	63.173

The magnetic depth calculation result (Table 1) shows that Curie isotherm depth varing from 19.18 to 30.95 km with an average of 23.12 km. Also, the geothermal gradient ranges from 21.98 to 30.95 ^{o}C/km, with an average of 25.27 ^{o}C/km. The Heat flow (flux) obtained varies from 51.95 to 77.37 mWm^{2} with an average of 63.17 mWm^{2}.

From the depth calculations using spectral analysis, two anomalous depth sources were interpreted. The deeply seated magnetic anomalous sources varying from 1.91 to 3.78 km, and shallower seated magnetic anomalous sources which ranges from 0.98 to 1.98 km (Fig. 11). Deeply seated magnetic anomalous sources may possibly denote depth to the basal crystalline rocks, while the shallower seated magnetic anomalous sources maybe associated with intrusive igneous and/or magnetized bodies coved

by sediment. The basal depth is abysmal in the entire south and central part of the study area, whereas, at other parts of the area such as Kutawenji, Lafiaji, Koton-Karfi and Lapai areas have shallower sources.

More so, the 3-D surface plot of depth to the top of the anomalous magnetic body shows presence of peaks (uplifts) and depressions (troughs). Around Agaje, Egbako, Olle, Mopa and Abaji areas, there visible linear depressions and these areas reveal higher sediments than the other parts such as Kutaeregi, Paiko, Lapai, Lafiagi, Aiyegunle, and Koton-Karfi areas which have prevalent uplifts (peaks) in conjunction with lower sedimentary thicknesses (Fig. 12). The presence of these peaks (uplifts) suggests that there are numerous intrusive bodies around these areas; as a result, there are more tectonic activities in the areas associated with depressional feature. According to Biswas et al, (2016 and 2017) and also Biswas (2015), these identified igneous intrusives generally occur as silly and dykes.

Prevalent Intrusive sources and Geologic model across a profile in the area

The geologic model (Fig. 13 and 14) obtained from the quantitative interpretation of the residual magnetic data reveals four geological stages namely: sedimentary stage, ferromagnetic bodies, paramagnetic bodies and lower crust bodies. The sedimentary infilling along this profile has a variable thickness which ranges from 0.20- 3.21 km. The deepest sedimentary cover occurs at the eastern and western ends of the profile (Egbe) (Fig. 14a) while the shallowest is at the middle. More so, the ferromagnetic bodies underlain the sedimentary layer and it has an average thickness of 6.1 km, the depth to the ferromagnetic bodies range from 12.04 to 13.0 km in this profile. Also, the paramagnetic bodies which are associated with Curie point depths and upper mantle have depth range of 13.10 to 24.01 km. It is believe that the heat from the mantle must have reworked the magnetic body making them to loss the magnetism. The model suggests that the deepest Curie point depth occurs in both left and right hand side of the model while at the middle, the Curie point depth is shallowest. The model interpretation is also shown in Fig. 14b.

Core Sample Analysis and Its Implication around Koton-Karfi

Core sample analysis within Koton-Karfi reveals different lithologic units within the sample locations. The depth to the oolitic iron ore obtained across the area ranges from 20.79 to 101.2m with an average of 38.52m (Table 2).

Table 2
Oolitic Iron Ore Deposit Level with respect to Mean Sea Level (MSL)

Borehole Co-Ordinates	Elevation (m)	Borehole Depth (m)	Oolitic Ore Deposit level w.r.t. MSL (m)
N08^{0}09’305” E006050’48.1”	260	42.56	217.44
N08^{0}09’305” E006050’48.1”	263	35.2	227.8
N08^{0}09’30.7” E006051’12.6”	267	39.68	227.32
N08^{0}09’30.7” E006051’208”	269	42.82	226.18
N08^{0}09’22.3” E006050’482”	259	42.65	216.35
N08^{0}09’22.4” E006050’56.4”	258	39.34	218.66
N08^{0}09’22.4” E006051’12.7”	266	39.33	226.67
N08^{0}09’22.7” E006051’20.8”	275	42.38	232.62
N08^{0}09’22.7” E006051’20.8”	271	42.59	228.41
N08^{0}09’14.2” E006050’48.3”	243	42.62	200.38
N08^{0}09’14.9” E006051’04.7”	265	42.37	222.63
N08^{0}09’06.1” E006050’56.4”	266	42.34	223.66
N08^{0}09’06.1” E006051’04.7”	266	40.32	225.68
N08^{0}09’0.63” E006051’12.9”	270	41.61	228.39
N08^{0}09’0.64” E006051’21.1”	265	42.61	222.39
N08^{0}08’58.0” E006050’56.4”	283	40.45	242.55
N08^{0}08’58.1” E006051’04.8”	262	42.61	219.39
N08^{0}08’58.2” E006051’13.1”	254	24.05	229.95
N08^{0}08’58.1” E006051’21.0”	250	20.79	229.21
N08^{0}08’58.0” E006050’48.4”	262	25.53	236.47
N08^{0}09’06.09” E006050’48.3”	270	20.79	249.21

Borehole Co-Ordinates	Elevation (m)	Borehole Depth (m)	Oolitic Ore Deposit level w.r.t. MSL (m)
N08^{0}09'14.2" E006051'56.4"	265	23.05	241.95
N08^{0}09'14.3" E006051'12.6"	284	23.05	260.95
N08^{0}09'14.5" E006051'21.1"	258	23.05	234.95
N08^{0}09'30.6" E006050'56.2"	229	101.2	127.8
Average	263.20	38.52	224.68

The elevation map of Koton-Karfi area (Fig. 15) was produced for effective correlation with the ooolitic iron ore level map (Fig. 15). Nevertheless, the ooolitic iron ore level with respect to mean sea level across Koton-Karfi area were computed by subtracting depths to oolitic iron ore layers deduced from the core drilling from surface elevations obtained during the data acquisition (Table 2). Thus, maps of the oolitic iron ore levels with respect to elevations were generated in order to depict the possible trend of the oolitic iron ore level across the study area (Fig. 16). Considering elevation and oolitic iron ore maps of Koton-Karfi area (Figs. 15 and 16), it is evident that the trend of the oolitic iron ore level is predominantly in NE-SW direction and mineralogically, the mineralization will flow this trend.

More so, Fig. 15 reveals that the anomalous body level (Ooilitic iron ore level) is deep around northeast and southwestern parts of Koton-Karfi; whereas at northwestern part of Koton-Karfi, the depth to the anomalous body (Ooilitic iron ore) is shallow with average oolitic iron ore deposit level as 225m.

Furthermore, profiles running from T-T^I at Fig. 14 and U-U^I at Fig. 15 were superimposed in order to establish the variation phenomenon across the area. Here, it was observed that the oolitic iron ore level follows the topographical level which implies that the topography controls the configuration of the iron ore level (Fig. 17).

Result from qualitative interpretation reveals that the area is extremely fractured, with fractures trending NE-SW direction and minor ones in NW-SE and E-W directions, the trend of these structures is in conformity with the trend of structures within the Nupe basin. These fractures can serve as migrating pathway for both geothermal energy flow and fluids like hydrocarbon. The work of Ojonugwa et al, (2018) believes that the stratified nature of the carbonaceous shale with intercalated sandstone found within the study area may probably favour fluid migration into potential reservoir rocks that are made up mostly of fluvial deposit, flood plain and shelf sandstones of the Lokoja and the Patti Formations.

Quantitatively, the depth to the top of magnetic basement rock (sedimentary thickness) within the study area have been delineated along seven different profile lines using Peter's half slope and Spectral analysis of aeromagnetic data and the result shows two depth model across the area, namely; the shallower magnetic sources which vary from 0.56 to 1.96 km and the deeper magnetic sources which

vary from 2.01 to 4.27 km. The Curie isotherm depth result revealed deeper depth at Kutiwenji, Egbako, Lapai, Paiko, Olle, Mapo and Baro areas, ranging from 22.60 to 27.91 km, in other parts, the Curie isotherm depth was shallower and ranged from 19.18 to 22.20 km. The calculated thermomagnetic properties reveals average values of 23.12 km Curie isotherm depth, 25.27 ^{o}C/km geothermal gradients and 63.17 mWm^{2} heat flows in the area.

Result from the core drill data reveals that the anomalous body level (Ooilitic iron ore level) is deep around northeast and southwestern parts of Koton-Karfi; whereas at northwestern part of Koton-Karfi, the depth to the anomalous body (Ooilitic iron ore) is shallow with average oolitic iron ore deposit level as 225m.

Integrating all the results and deductions obtained in this work, it can be deduce that those regions (such as Baro, Kutaeregi, Kutiwenji and Koton-karif) with shallow or low sedimentary thicknesses are possible areas that are associated with magnetic mineral ore deposits like oolitic iron ore identified in Koton-Karfi area (Fig. 18). Actually, these areas might not support hydrocarbon generation.

However, the sedimentary infillings around Pategi, Agaje, Olle and Baro area is relatively high in conjunction with the high geothermal gradient and heat flow; will possibly pave way for hydrocarbon potential in this area provided that all other conditions for hydrocarbon generation is available. Previous workers such as, Ikumbur et al, (2013), Okubo et al, (1985), Adeleye. (1974), Ojo and Akande (2012) suggest that the study area contains carbonaceous shales intercalated with sandstone and clay, which is a potential source rock.

5. Conclusions

The qualitative interpretation of the TMI data and residual anomalous data shows a complex configuration of magnetic signatures of the wavelengths. This varying amplitude of the anomalous bodies denotes change in magnetic intensities from diverse acoustic sources and it evident in the study area (such as magnetic intensity range between 7200 nT and 8500 nT). Around Paiko, Kutaeregi, Koton-karfi, Bida, Lapai, Agaje, and Aiyegunle areas, The TMI and residual anomalous maps shows the underlying basement as having magnetic intensities range ranges from 7500 to 8460 nT and -220 to 240 nT respectively. There are strong evidences of igneous intrusion when juxtaposed with the geologic map of the area. However, at the central parts (Pategi, Baro, Gulu, Lafiagi areas) and beyond, the contour lines are extensively spaced indicating that the sedimentary infilling within these areas is thick. We then conclude that the widely spaced contours in conjunction with the high magnetic acoustic field intensity values interpreted may have been related to the vein bearing mineral and this affirmation is reinforced by the geologic information of the study.

The 3D structural model shows the presence of uplifts and depressions, a characteristic manifestation of secondary structural feature named folds. Lineament alignment in the area was produced from the residual anomalous magnetic data. The main structural trends were NE-SW with minor E-W and NW-SE

trends. Juxtaposing these lineaments on the geological of the area, it shows high concentration of structural lineament in area with intense tectonic activities which was believed to be due to intrusive igneous bodies while the less concentrated area fall around zone of high sedimentary infillings suggesting deeply seated basement rock.

The structural configuration of the study area is in conformity with the trend of structures within the basin which trend NE-SW and NNE-SSW as prominent trend, and E-W, NW-SE, and W-E are the minor trends. Previous researchers have established that these obtained trends NE-SW NNE-SSW and NW-SE within the study area are as a result of Pan-African Orogeny while the E-W may perhaps be Pre-Pan-African Orogeny.

Quantitative result revealed a two depth model; the shallower seated anomaly varied from 0.56 to 1.96km (for Peter's slope method), and for spectral analysis, the shallower bodies varies from m 1.27 to 1.96km; the deeper bodies varies from 2.01 to 3.27km (for Peter's slope method) while for spectral analysis, the shallower bodies varies from 2.01 to 4.27km. However, for the depth to the centroid obtained through the spectral analysis depicts depth ranges from 9.79 to 15.75km across the study area. The depths to the top of magnetic anomalies obtained through spectral analysis were used to identify the prevalent intrusive bodies along the magnetic profiles. This result is in conformity with earlier works done within Nupe Basin and portions of the adjoining basement. The northeastern and southern parts of the study area have evidence of huge igneous intrusives and it is believed that the basement rocks of the central Nigeria might have intruded within and around the study area.

Furthermore, the model map of depth to the centroid reveals higher depth values at areas like Kutiwenji, Egbako, Lapai, Paiko, Baro, Mopa and Olle while lower values are recorded at Lafiagi, Isanlu-Esa, Gulu and Abaji. The 3-D surface plot of the Curie isotherm depth shows presence of peaks (uplifts) and depressions (troughs) across the study area. Around Kutiwenji, Egbako, Lapai, Paiko, Baro, Mopa, Agaje, and Olle areas, there are visible linear depressions and these areas reveal higher depth to the Curie point isotherm than the other parts such as Lafiagi, Isanlu-Esa, Gulu and Abaji areas which have prevalent uplifts (peaks) in conjunction with lower values. At the northern and southern axes (Kutiwenji, Kutaeregi, Paiko, Lapai, Egbako, Mapo, and Olle), the geothermal gradient thickness is lower compare to the other areas (Fig. 16). At Lafiagi Isanlu-Esa, Egbe, Abaji and Gulu areas, geothermal gradient have relatively high geothermal gradient ranging between 25.76 and 30.95^{o}C/km averaging 25.27 ^{o}C/km.

Core sample analysis within some parts of the study area reveals that depth to top of the oolitic iron ore across the area ranges from 20.79 to 101.2m with an average of 38.52m. Thus, maps of the oolitic iron ore levels with respect to elevations were generated in order to depict the possibly trend of the oolitic iron ore level across the study area to be predominantly in NE-SW direction and mineralogical, the mineralization will flow this trend.

Declarations

Acknowledgments

We appreciated and thank the National Geological Survey Agency, Abuja Nigeria, for providing the input Aeromagnetic data and National mines for providing the core sample.

Competing Interest

There is no conflict of interest in this work. All the finance used in the work is from the author and coauthors. We also declared that no part of this work has been publish or under any consideration in any journal.

Authors Contribution

A. Usman Ayatu Ojonugwa is the lead researcher. He did the interpretation, depth calculations and modelling
B. Chinwuko Augustine Ifeanyi help also in the interpretation and editing of the work
C. Azuoko George Best did the type setting work and he was part of the interpretation
D. Chima Chizoba did the depth calculation and was part of the team that did the interpretation of the core sample

References

1. Abraham EM, lawal KM, Ekwe AC, Alile O, Murana ka, Lawal AA. (2014) Spectral analysis of aeromagnetic data for geothermal energy investigation of Ikogosi warm Spring-Ekiti state, Southwestern Nigeria. Geotherm Energy; 26: 1-21.
2. Adeleye, D.R. (1974). Sedimentology of the fluvial Bida Sandstone (Cretaceous), Nigeria. Elsevier journals of Sedimentary Geology, vol. 12, no. 1, pp. 1-24.
3. Akande, S.O., Ojo, O.J and Ladipo, K.O. (2005). Upper cretaceous sequences in the Southern Bida Basin, Nigeria. Mosuro publishers, 5 Oluware Obasa Street, Bodija, Ibadan, Nigeria. pp. 78
4. Anakwuba, E. K., and Chinwuko, A. I. (2015). One Dimensional Spectral Analysis and Curie Depth Isotherm of Eastern Chad Basin, Nigeria. Journal of Natural Sciences Research, vol.5, no.19, pp.14-22
5. Biswas, A., Parija, M. P., Kumar, S. (2017). Global nonlinear optimization for the interpretation of source parameters from total gradient of gravity and magnetic anomalies caused by thin dyke. Annals of Geophysics, 60 (2), G0218, pp 1-17.
6. Biswas, A., Acharya, T. (2016). A Very Fast Simulated Annealing method for inversion of magnetic anomaly over semi-infinite vertical rod-type structure. Modeling Earth Systems and Environment, 2(4), pp 1-10
7. Biswas, A. (2015). Interpretation of residual gravity anomaly caused by a simple shaped body using very fast simulated annealing global optimization. Geoscience Frontiers, 6(6), pp 875-893.
8. Bhattacharryya, B.K., and Leu, L.K. (1975). Spectral analysis of gravity and Magnetic anomalies due two dimensional structures. Geophysics, vol. 40, pp. 993-1031.

9. Chinwuko A.I., Usman, A.O., Onwuemesi A.G., Anakwuba, E.K., Okonkwo, C.C., and Ikumbur, E.B., (2014). Interpretations of aeromagnetic data over Lokoja and environs, Nigeria. International Journal of Advanced Geosciences, vol. 2, no. 2, pp. 66- 71.
10. Chinwuko, A.I., Onwuemesi, A.G., Anakwuba, E.K., Onuba, L.N., and Nwokeabia, N.C. (2012). The Interpretation of Aeromagnetic Anomalies over parts of Upper Benue Trough and Southern Chad Basin, Nigeria. Advances in Applied Science Research, Vol. 3, no. 3, pp. 1757-1766.
11. Ikumbur, E. B., Onwuemesi, A. G., Anakwuba, E. K., Chinwuko, A. I., Usman, A.O., Okonkwo, C. C. (2013). Spectral Analysis of Aeromagnetic Data over Part of the Southern Bida basin, West-Central Nigeria. International Journal of Fundamental Physical Sciences, vol. 3, no. 2, pp. 27-31.
12. Mandal, A., Biswas, A., Mittal, S., Mohanty, W. K., Sharma, S. P. Sengupta, D., Sen, J., Bhatt, A. K. (2013). Geophysical anomalies associated with uranium mineralization from Beldih mine, South Purulia Shear Zone, India. Journal Geological Society of India, 82(6), pp 601-606.
13. Obaje, N.G.J, et al. (2013). Preliminary Integrated Hydrocarbon Prospectively Evaluation of the Bida Basin in North Central Nigeria. An International Journal, vol.3, no. 2, pp. 36-65.
14. Ojo, O.J and Akande, S.O. (2012) Sedimentary Facies Relationships and Depositional Environments of the Maastrichtian Enagi Formation, Northern Bida Basin, Nigeria. Journal of Geography and Geology. vol. 4, no. 1, pp. 136-147.
15. Ojonugwa Ayatu Usman, Ezeh CC, Chinwuko IA (2018) Integration of Aeromagnetic Interpretation and Induced Polarization Methods in Delineating Mineral Deposits and Basement Configuration within Southern Bida Basin, North-West Nigeria. J Geol Geophys 7: 449. doi: 10.4172/2381-8719.1000449
16. Okubo, Y.J., Graf, R., Hansen, R.O., Ogawa, K., Tsu, H., (1985). Curie point depth of the Island of Kyushu and surrounding areas. Japan Geophysicics, vol. 53, pp. 481-491.
17. Okonkwo, C. C., Onwuemesi, A. G., Anakwuba, E. K., Chinwuko, A. I., Ikumbur B. E. and Usman, A. O., (2012). Aeromagnetic Interpretation over Maiduguri and Environs of Southern Chad Basin, Nigeria. Journal of Earth Sciences and Geotechnical Engineering, vol.2, no. 3, pp. 77-93
18. Onwuemesi, A.G. (1995). Interpretation of magnetic anomalies from the Anambra Basin of southeastern Nigeria. Ph.D thesis, Nnamdi Azikiwe University Awka, Nigeria, pp.12-55.
19. Onwuemesi, A. G. (1997). One dimensional spectral analysis of aeromagnetic anomalies and curie depth isotherm in the Anambra Basin of Nigeria. Journal of Geodynamics, vol. 23, no. 2, pp. 95-107.
20. Ross, H.E., Blakely, R.J., and Zoback, M.D. (2006). Testing the use of aeromagnetic data for the determination of Curie depth in California. Geophysics, vol. 71, no. 5, pp. 51–59
21. Saibi, H, Aboud, E. and Azizi, M. (2015). Curie point depth map for Western Afghanistan deduced from the analysis of aeromagnetic data, Proceedings World Geothermal Congress 2015, Melbourne, Australia, pp. 19-25
22. Singh, A., Biswas, A. (2016). Application of global particle swarm optimization for inversion of residual gravity anomalies over geological bodies with idealized geometries. Natural Resources Research, 25(3), pp 297-314.

Figures

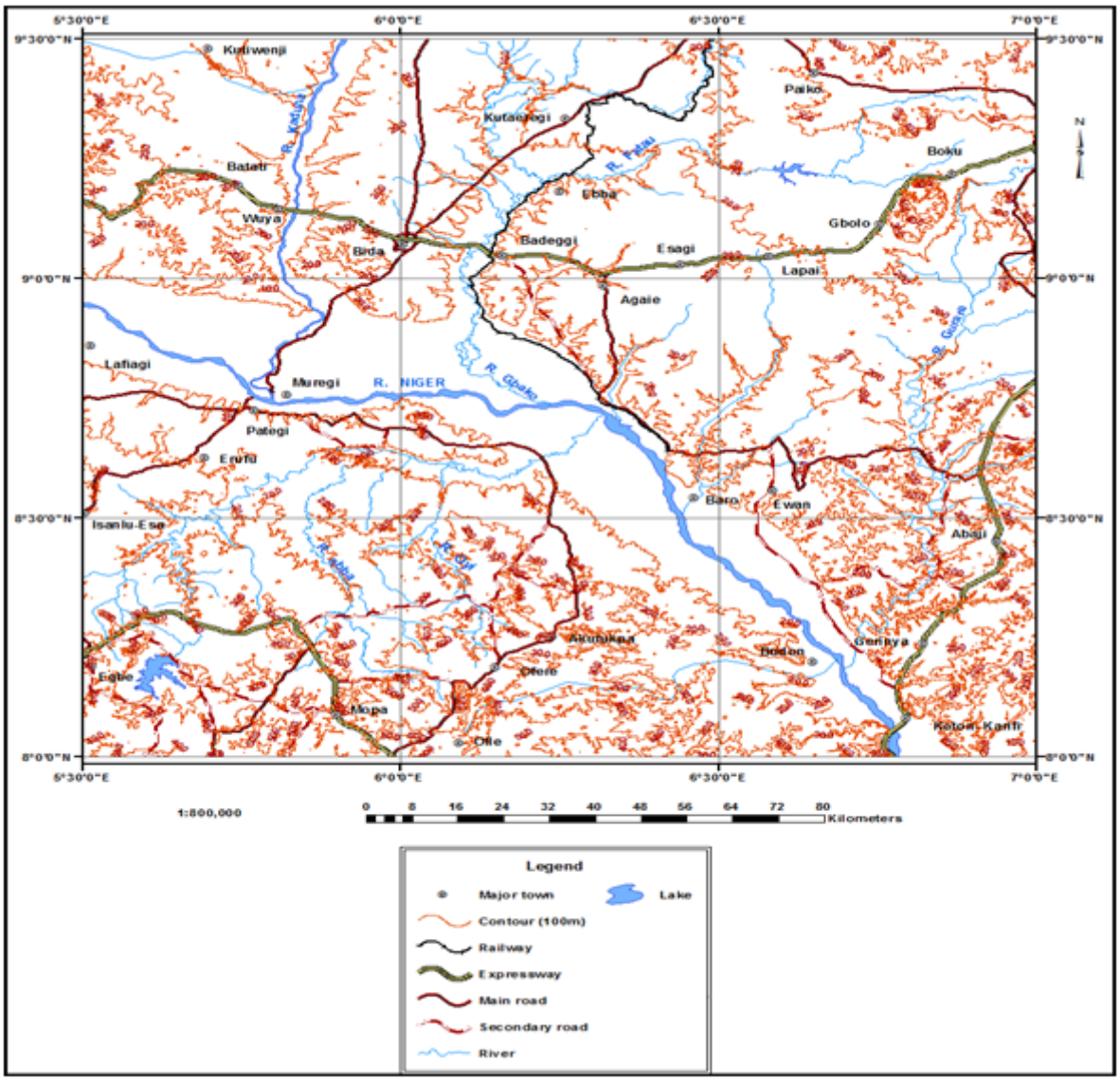

Figure 1

Accessibility Map of the Area

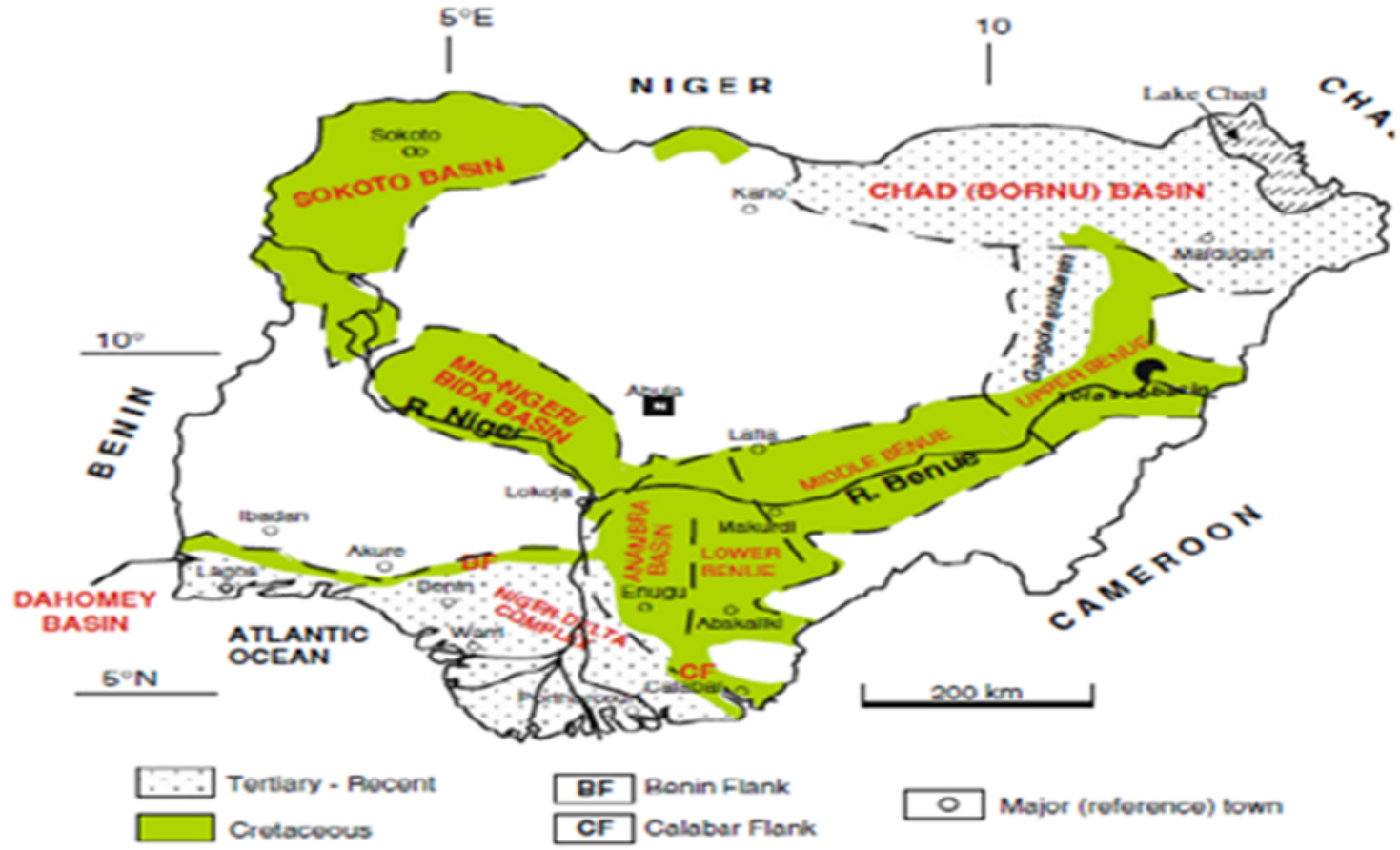

Figure 2

Locations of map area in the Geologic map of Nigeria (After Obaje *et al.*, 2013).

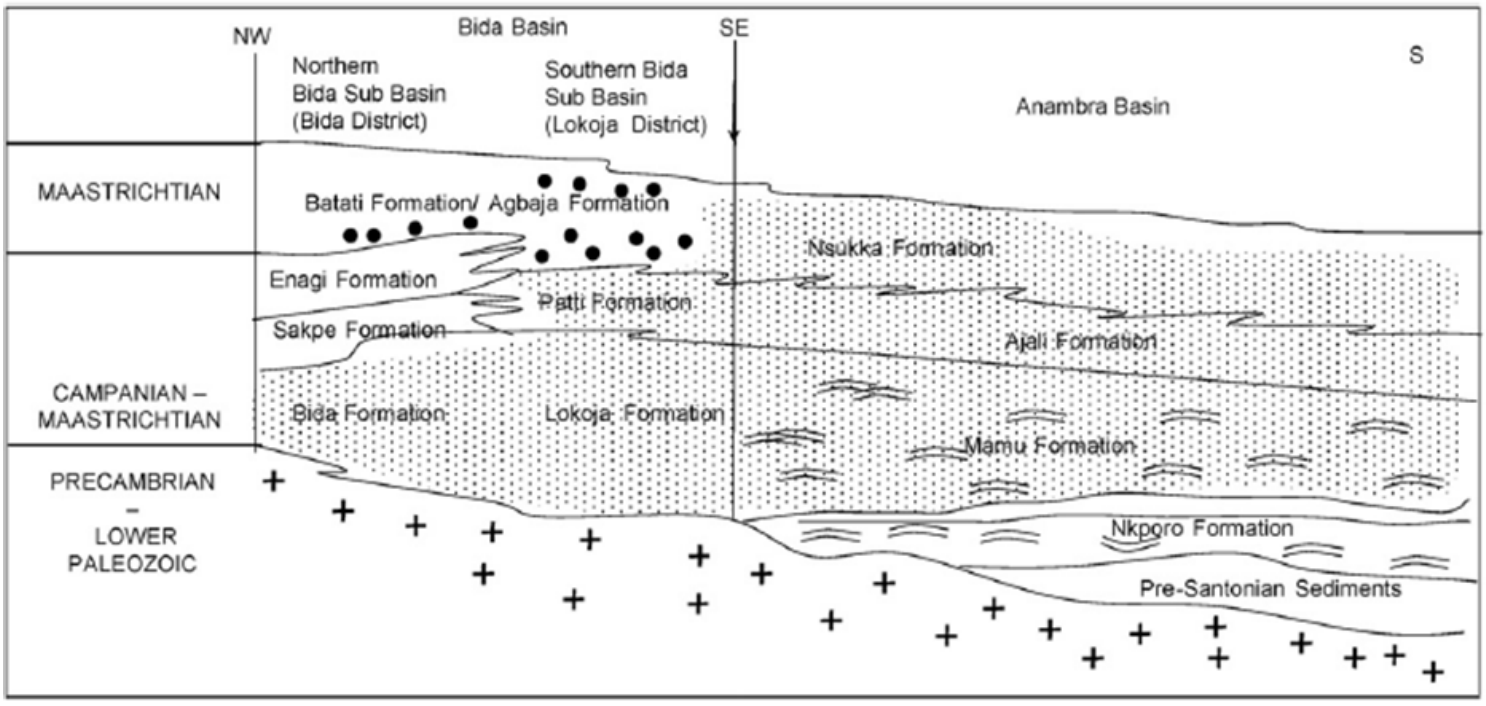

Figure 3

The Formation of southern Nupe Basin correlated with Anambra Basin (modified from Akande, *et al.,* 2005).

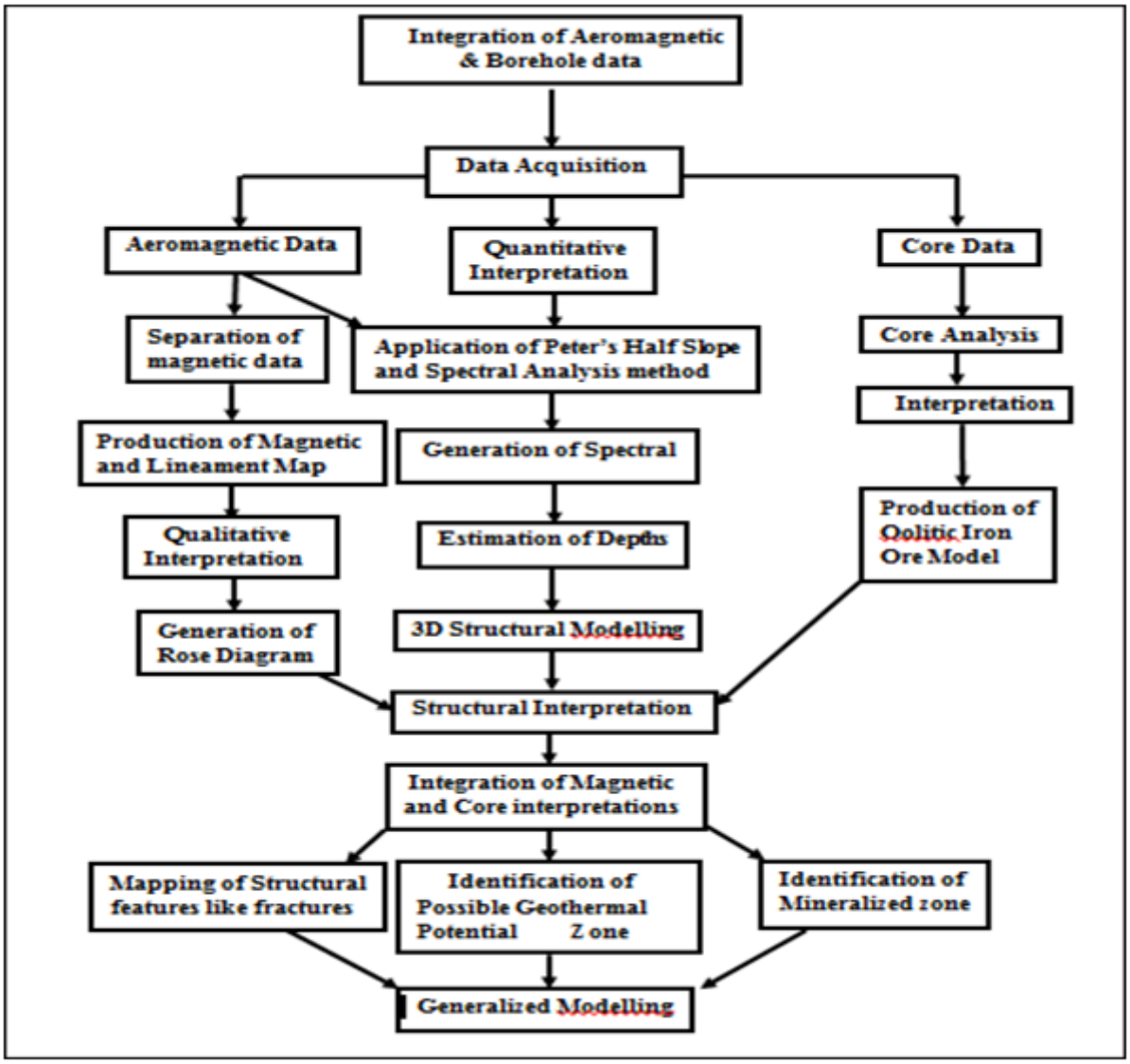

Figure 4

Research Workflow

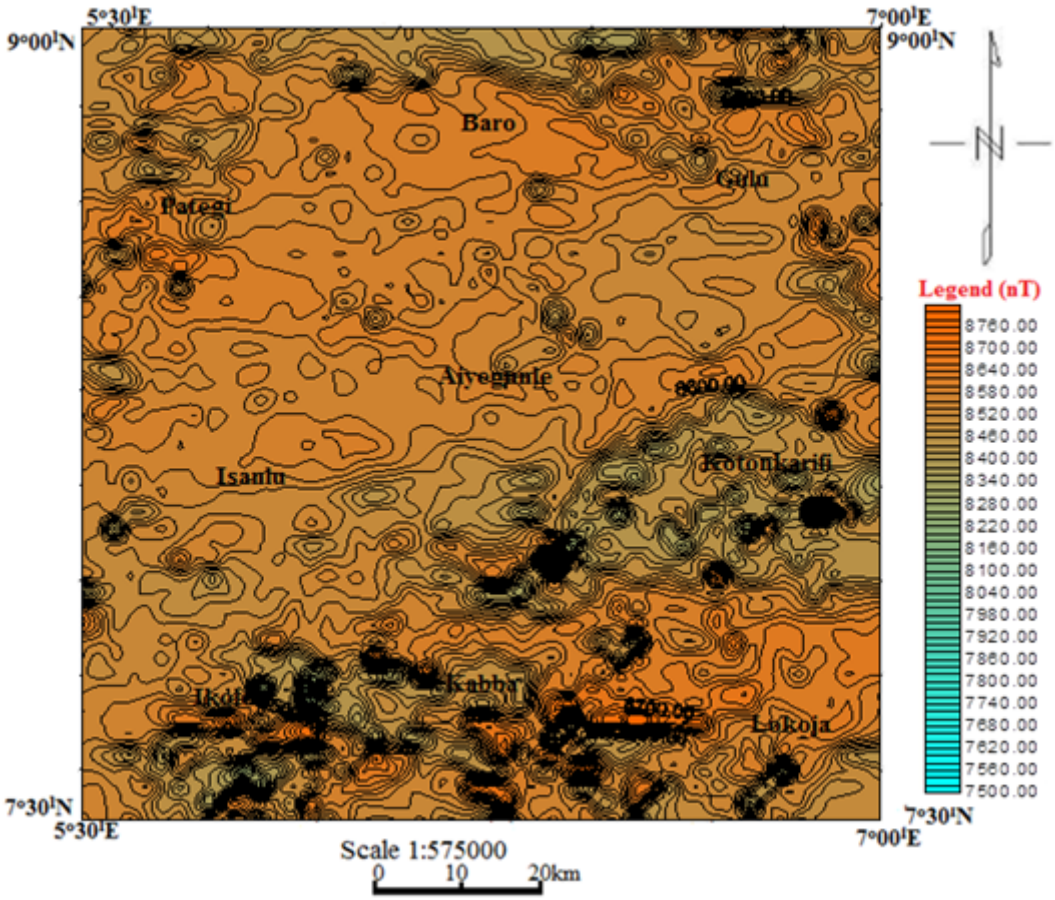

Figure 5

TMI Map of the Study area (Contour Interval~20nT)

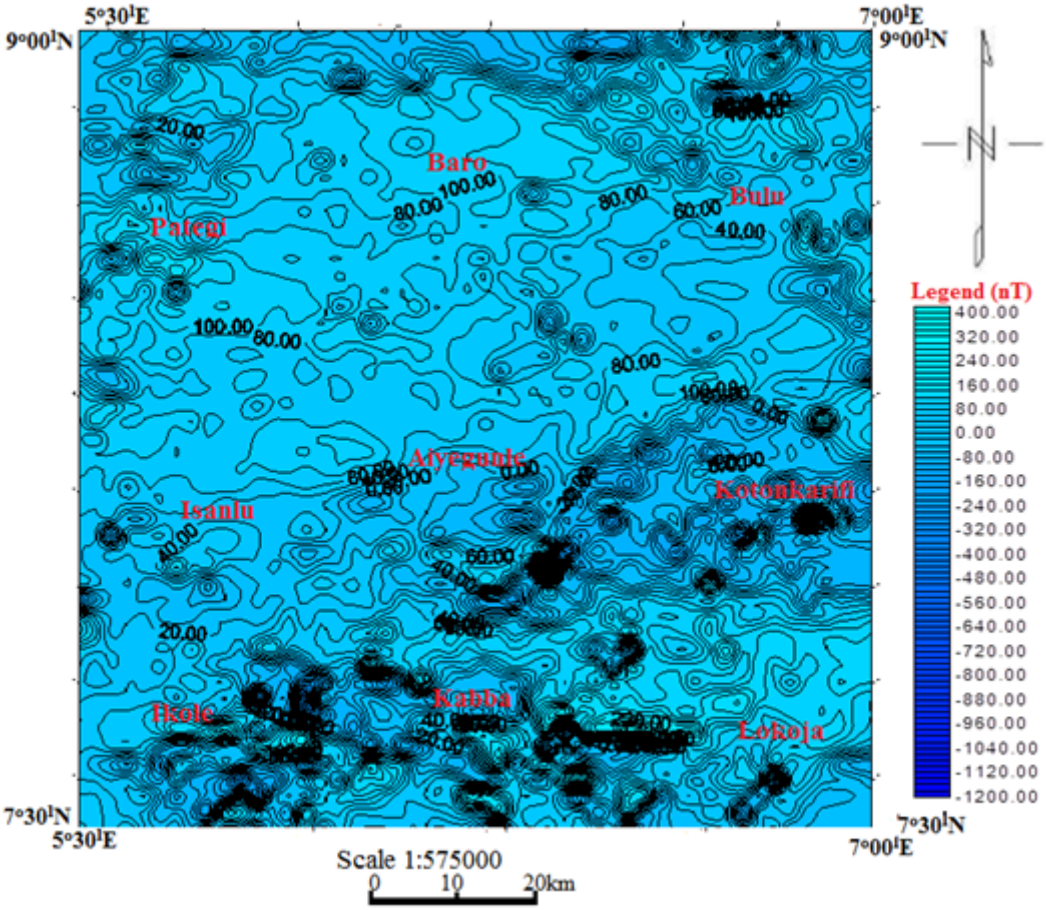

Figure 6

Residual Map of Bida and its Environs (Contour Interval~20nT)

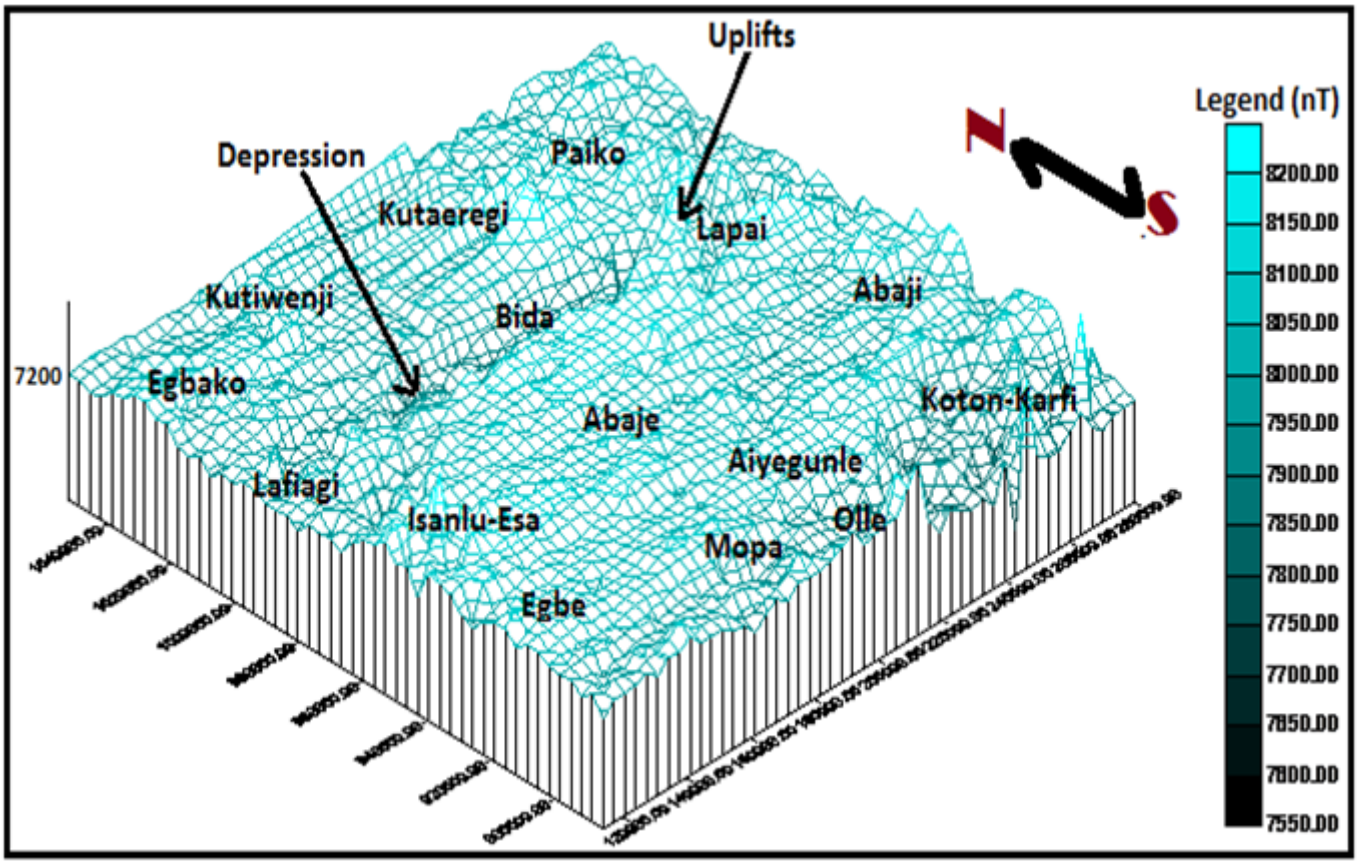

Figure 7

Real view distribution of total magnetic field intensity in the area

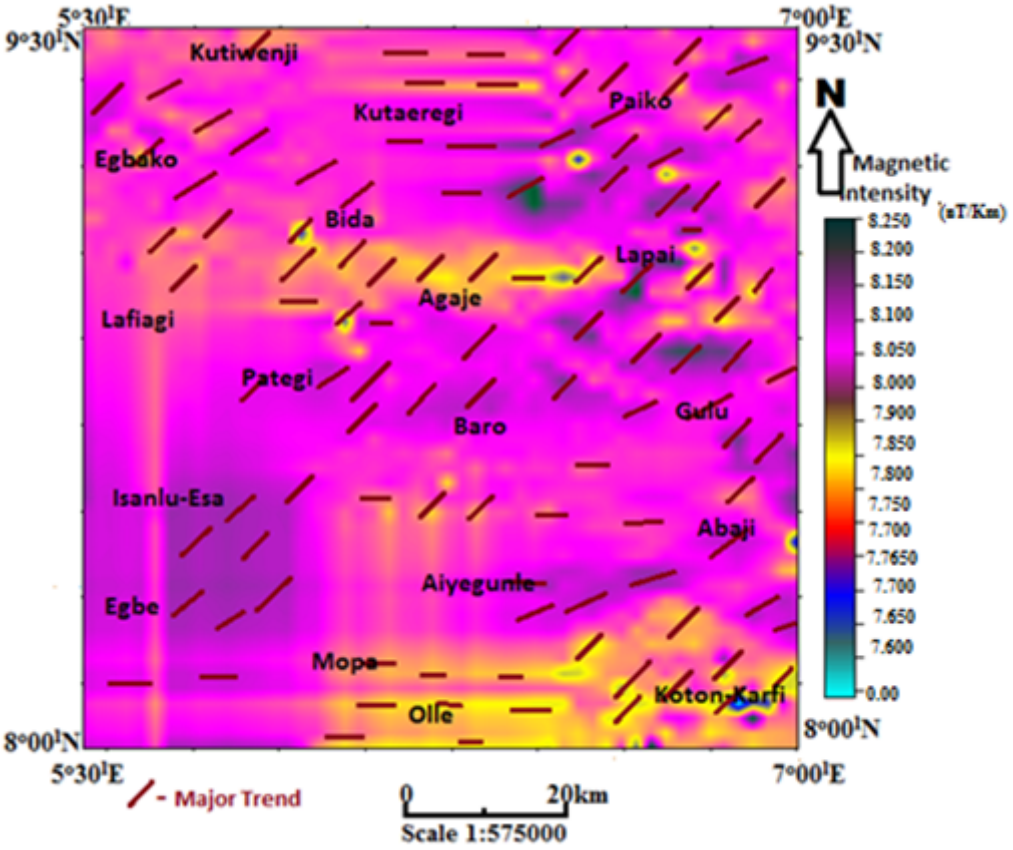

Figure 8

Analytical Map of the study the area

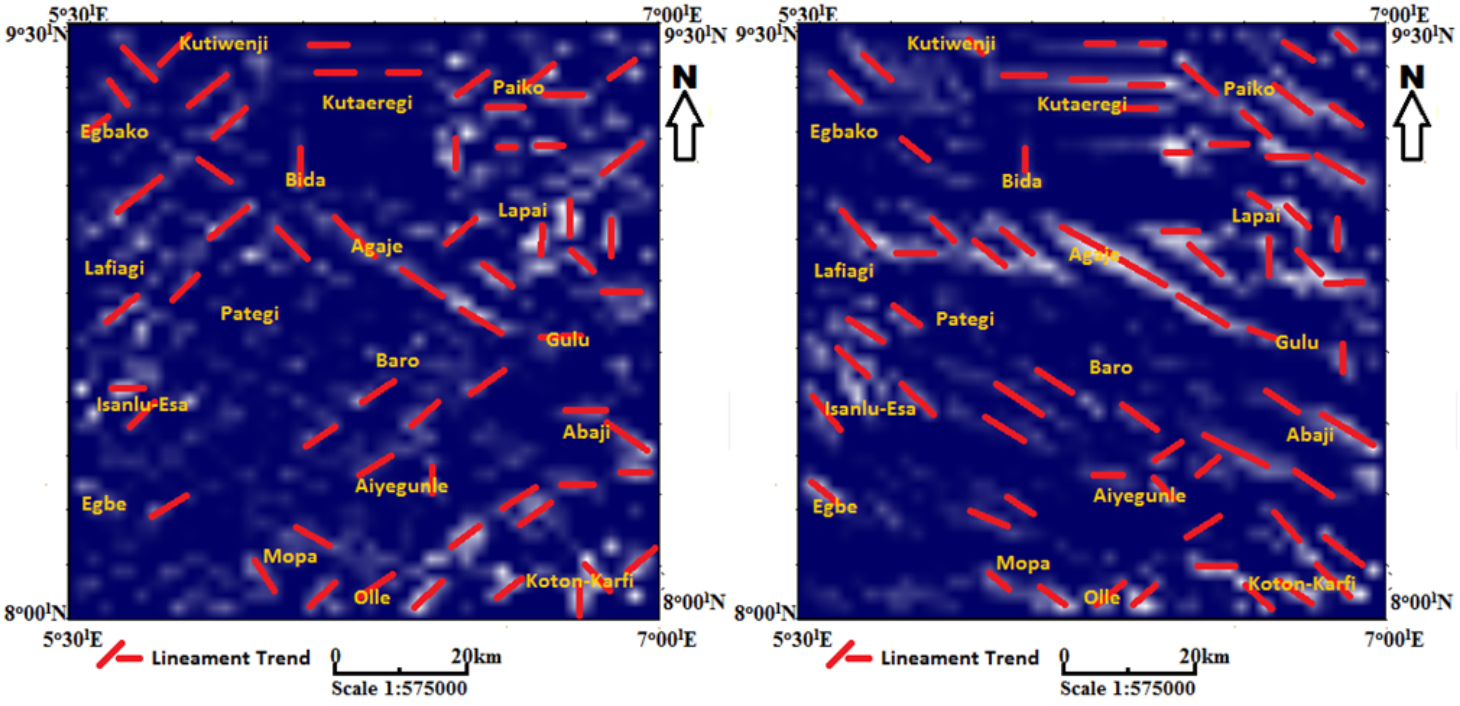

a) HPLA-0° and VPLA-0°

b) HPLA-45° and VPLA-0°

Figure 9

Residual Shaded intensity Field maps showing structural diection (HPLA-Horizontal Position Light Angle; VPLA-Vertical Position Light Angle)

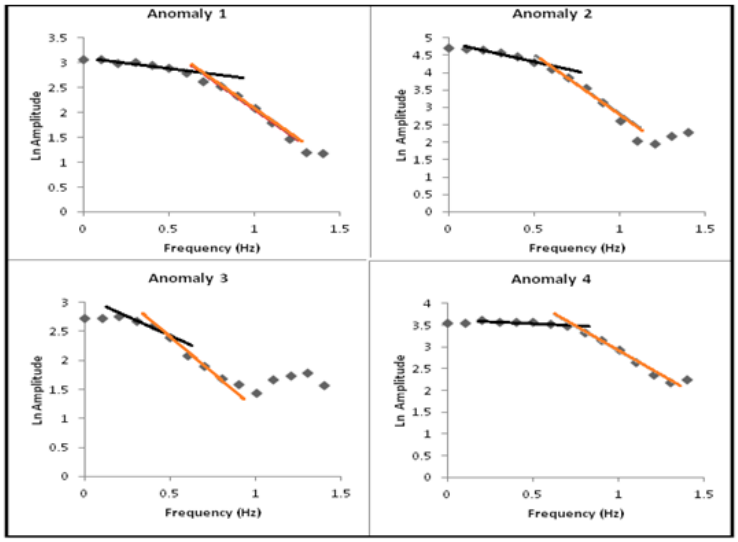

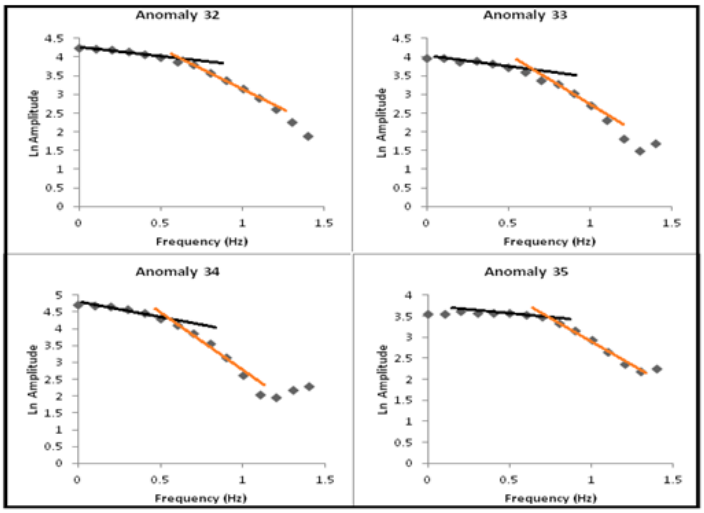

Figure 10

a and b: Representative spectral graph in the area.

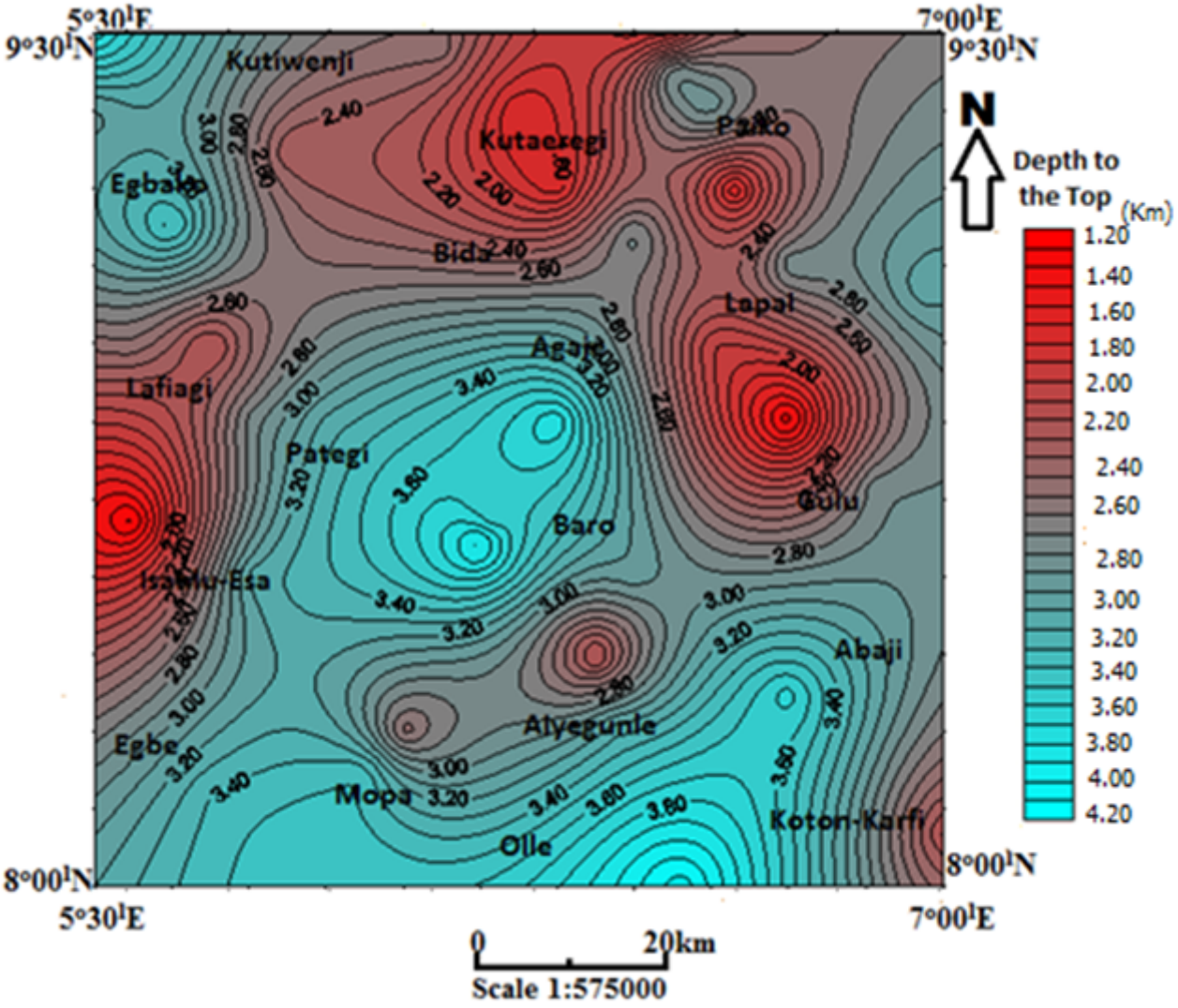

Figure 11

Basal depth (Contour Interval~0.1m)

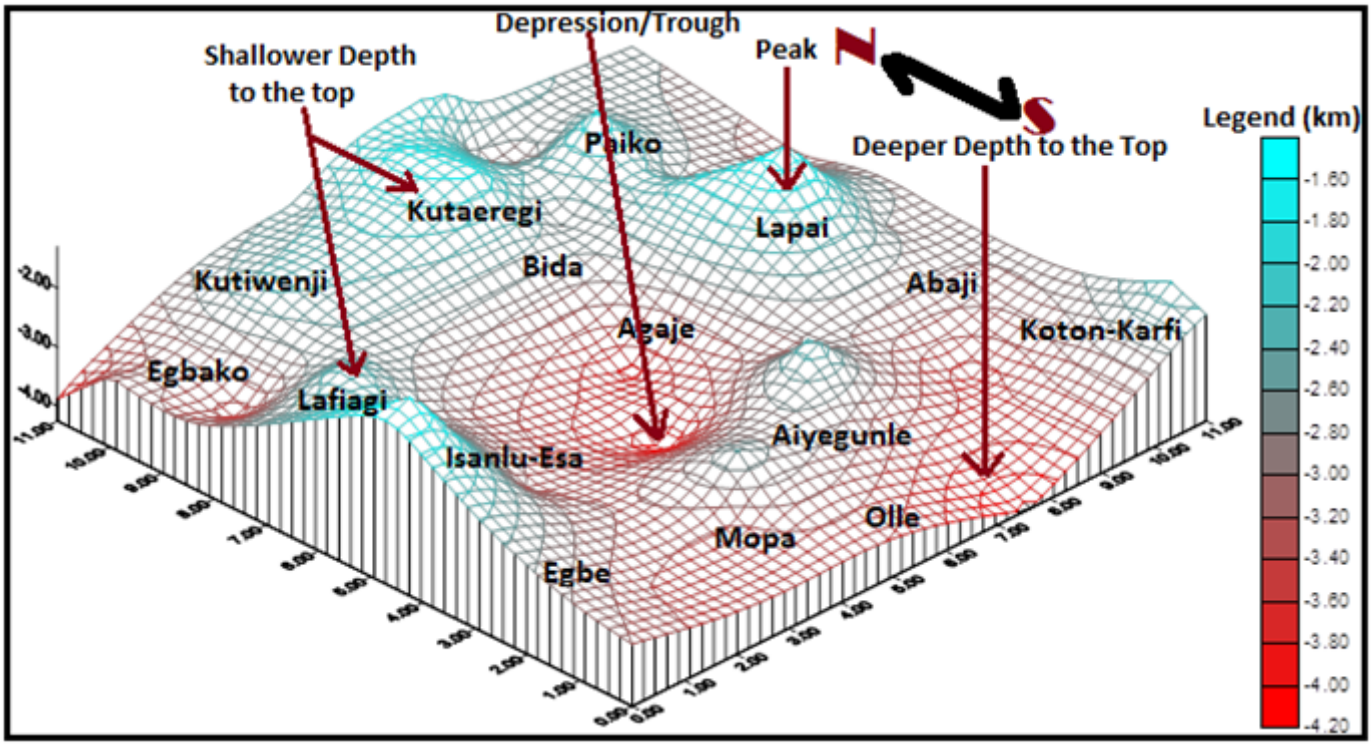

Figure 12

Real view model of depth to the top in the area

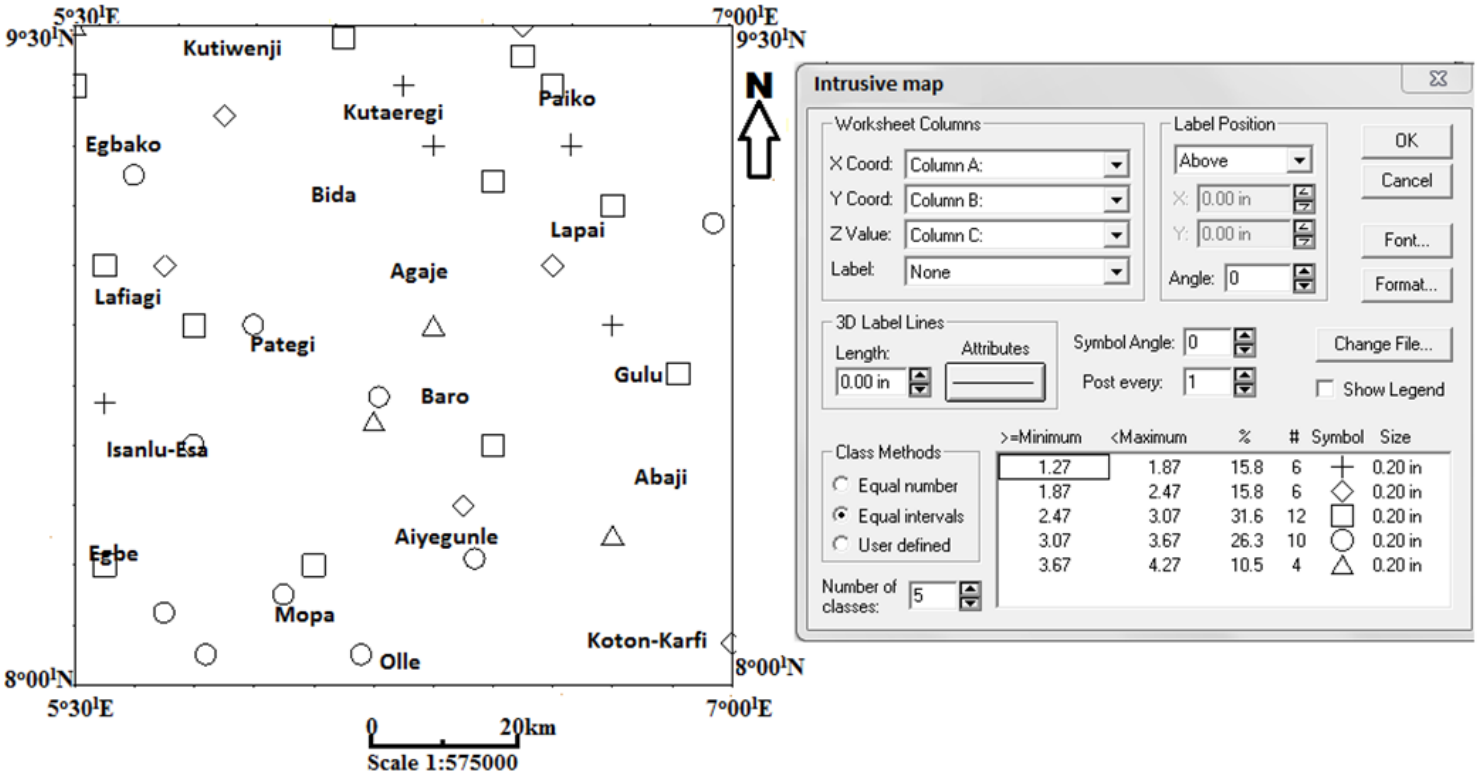

Figure 13

Prevalent Intrusive sources in the area

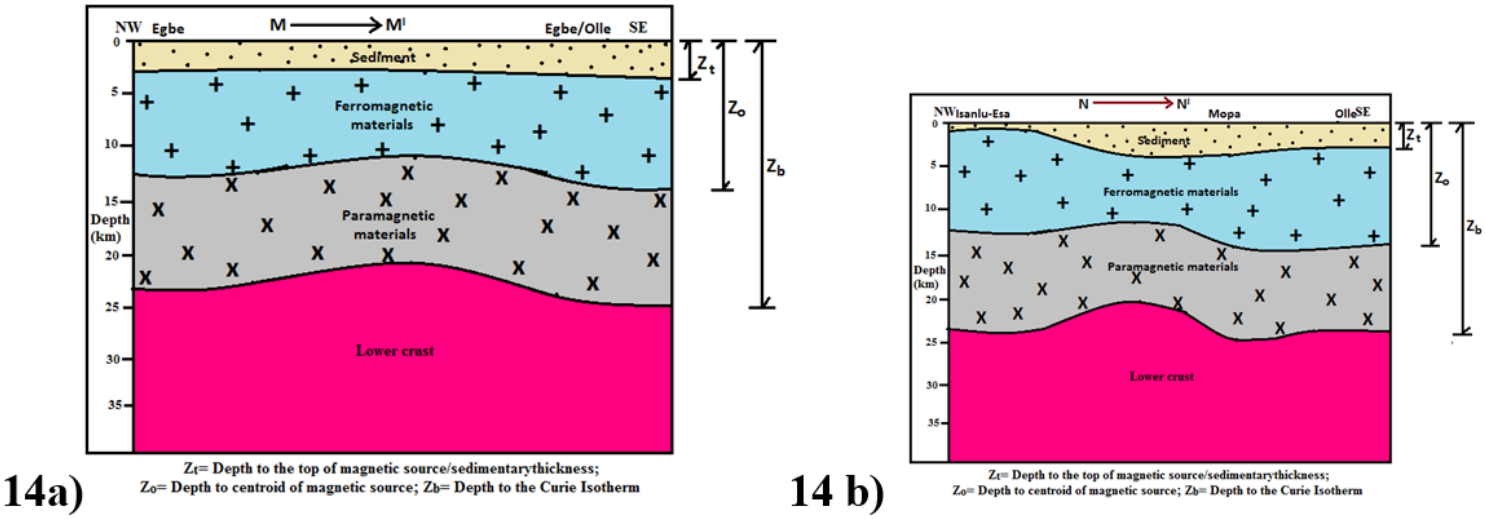

Figure 14

a and b: Curie isotherm depth modeling along Profile M-M^{l} and N-N^{1}in the study area

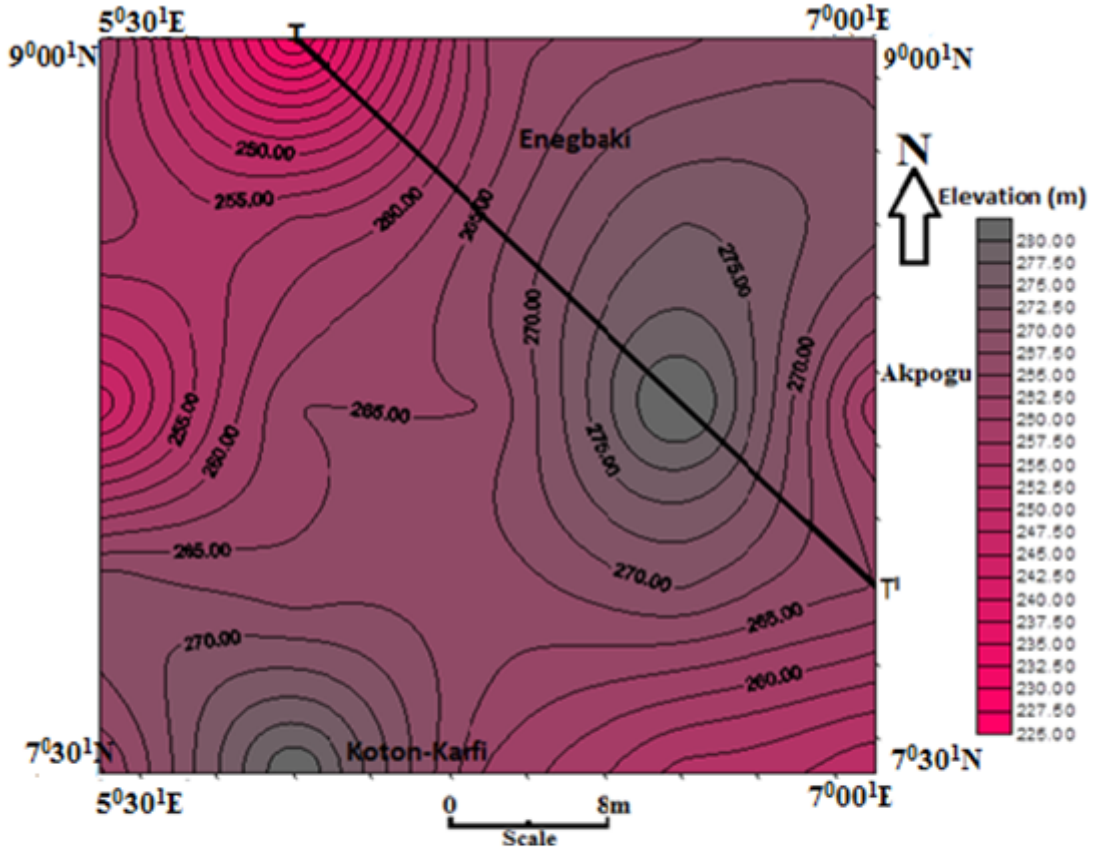

(Contour interval~2.5m)

Figure 15

Elevation Map of Koton-Karfi area

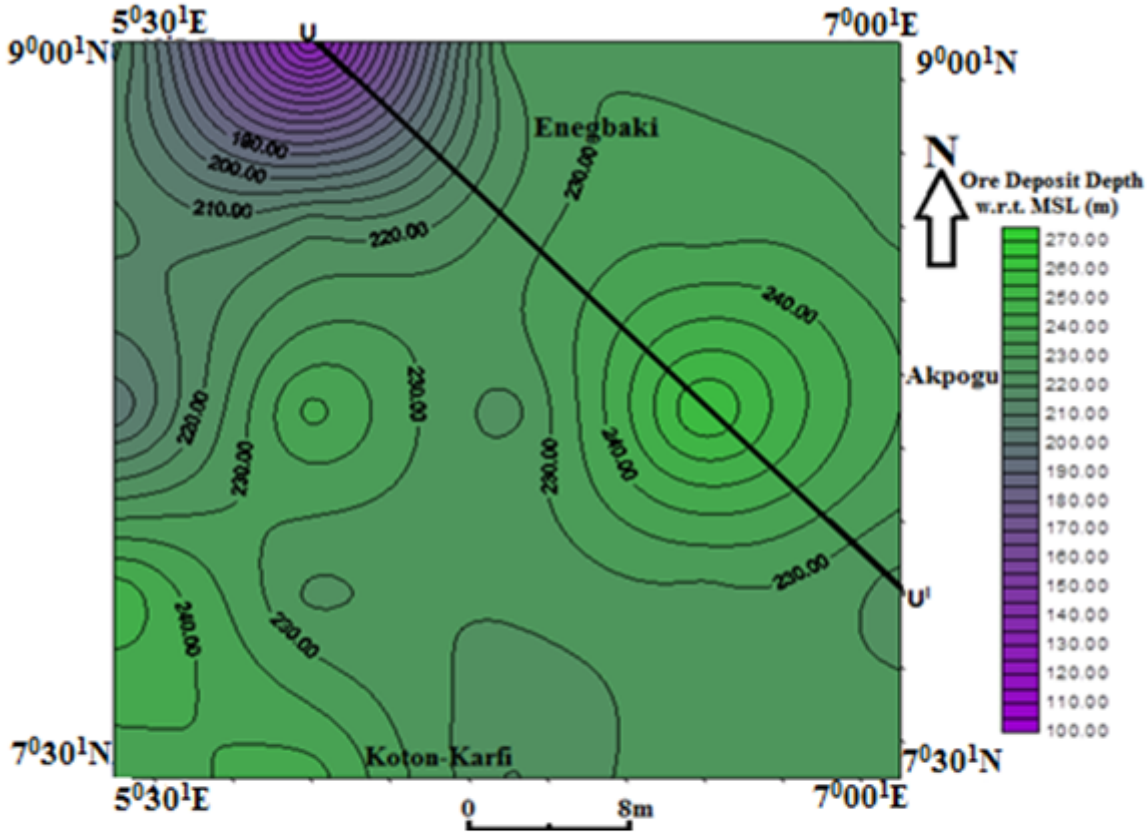

(Contour interval~5m)

Figure 16

Oolitic Iron Ore level of Koton-Karfi area

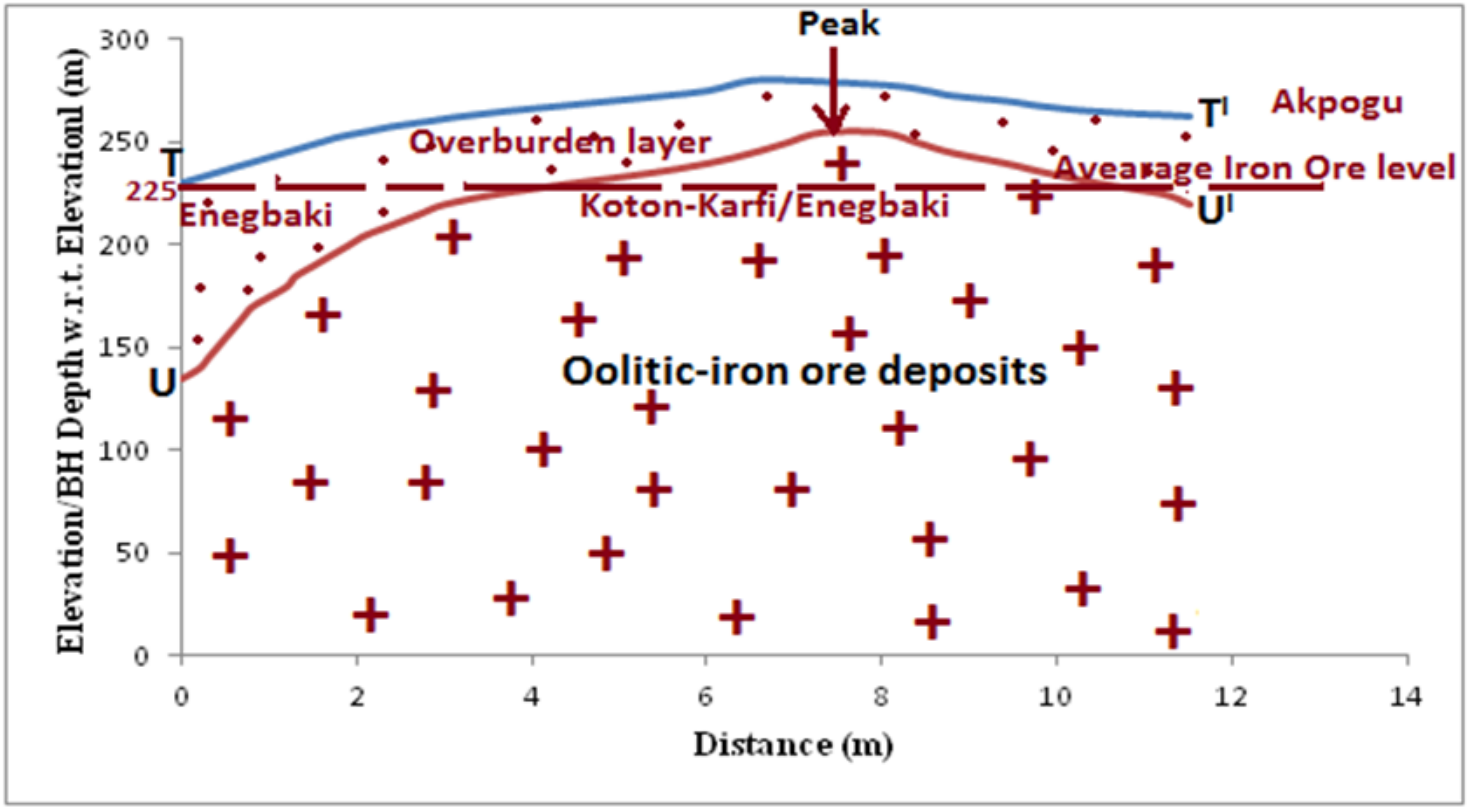

Figure 17

Juxtaposed topography and oolitic ore deposit level of Koton-Karfi area

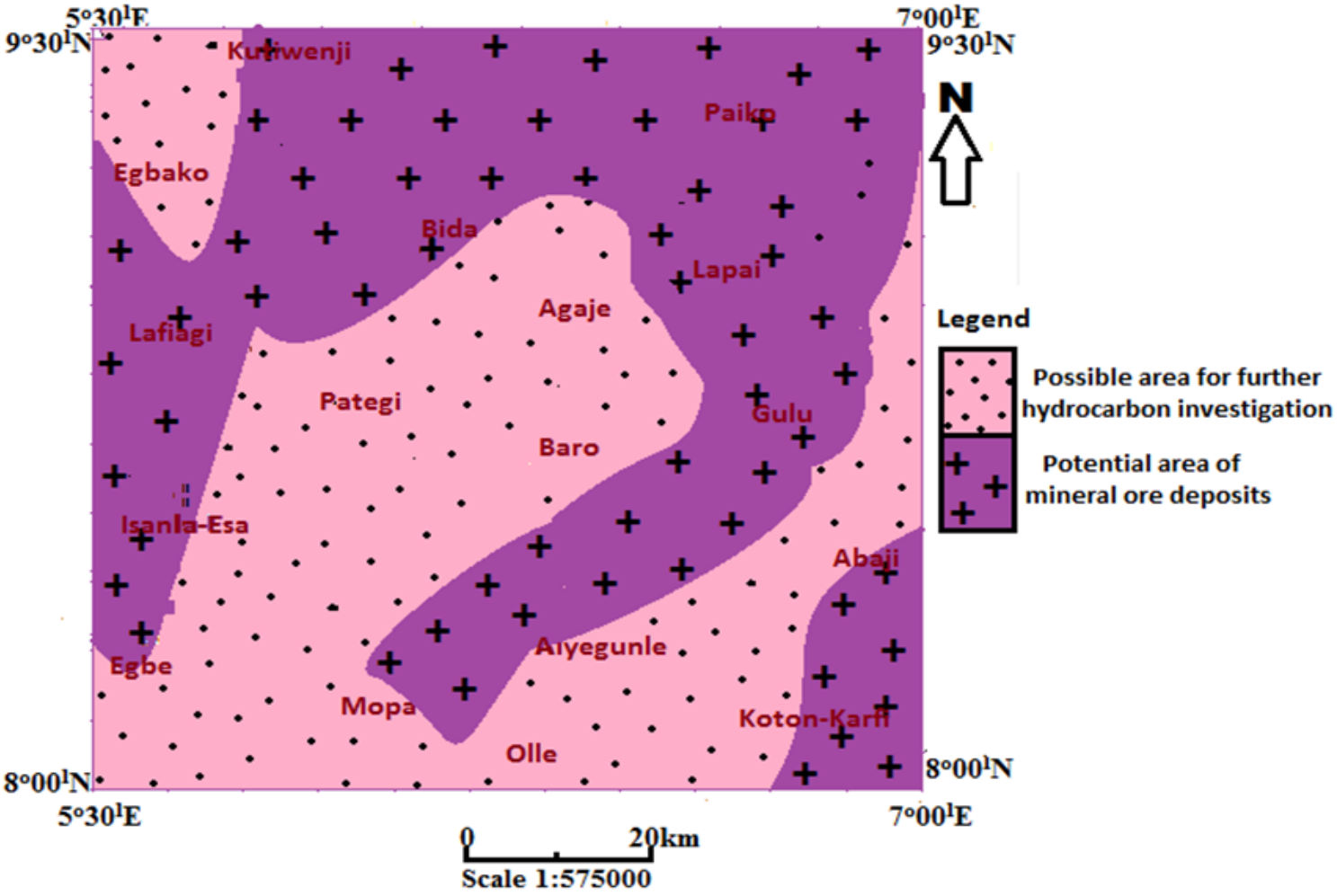

Figure 18

A generalized model for possible mineral deposits and hydrocarbon accumulation